



0021-9290(94)00087-5

TECHNICAL NOTE

NUMERICAL INSTABILITIES IN BONE REMODELING SIMULATIONS:
THE ADVANTAGES OF A NODE-BASED FINITE ELEMENT APPROACHChristopher R. Jacobs,*† Marc E. Levenston,*† Gary S. Beaupré,*†
Juan C. Simo† and Dennis R. Carter*†

*Rehabilitation Research and Development Center, Palo Alto V. A. Medical Center; †Department of Mechanical Engineering, Stanford University, California; and ‡Musculoskeletal Research Laboratory, Dept. of Orthopaedics, Pennsylvania State University, Hershey, Pennsylvania, U.S.A.

Abstract—Long bone structure occurs in two distinct forms. The bone mass near the joint is primarily found in a distributed, porous trabecular structure, while in the diaphyses a tubular cortical structure is formed. It seems likely that these two observed morphologies come about, at least in part, as a mechanical adaptation to the different mechanical demands in the two regions. Mathematical formulations of this dependency have been proposed, thus facilitating numerical simulations of bone adaptation. Recently two types of discontinuities have been observed in these simulations. The first type (near-field) appears in areas near distributed load application and is characterized by a 'checkerboard' pattern of density wherein adjacent remodeled elements alternate between low and high density. The second type of discontinuity (far-field) appears remote from the load application and is characterized by strut or column-like regions of elements which become fully compact bone while adjacent regions are fully resorbed. In fact, the far-field discontinuity is an accurate representation of bone physiology and morphology since it is consistent with the appearance of cortical bone in the diaphysis. On the other hand, the near-field discontinuity, appears in a region where continuous distributions of intermediate apparent densities (trabecular bone) are expected. This finding may cause some to question whether a single continuum formulation of bone remodeling can predict both discontinuous far-field behavior and continuous near-field behavior. We describe a node-based implementation of current continuum bone remodeling theories which eliminates the spurious near-field discontinuities and preserves the anatomically correct far-field discontinuities, thus indicating that a single biological process may be at work in forming and maintaining both far-field and near-field morphologies.

INTRODUCTION

The structure of long bones of the appendicular skeleton in the diaphysis is distinctly different from that seen adjacent to the bone ends. Bone morphology makes a dramatic transition from a distributed trabecular structure near the ends to a hollow cortical structure in the shaft. It has been proposed that this is a functional adaptation to the differing structural demands in the two regions (Curry, 1984). In particular, it is suggested that the purely cortical structures found in the diaphysis are well suited to the simple resultant loads in that region, while the more complex distributed loading applied near the joints are more efficiently supported by a continuous trabecular structure. It is well known that bone undergoes morphological changes in response to both increased and decreased mechanical demands by modifying external geometry as well as internal structure and many mathematical formulations have been proposed that relate these morphological changes to the local mechanical demands (Beaupré *et al.*, 1990b; Carter *et al.*, 1987; Cowin and Hegedus, 1976; Huiskes *et al.*, 1987; Kummer, 1972). This paper addresses stress-related internal bone remodeling only.

The advent of modern computer capabilities and numerical stress analysis techniques have allowed researchers to

relate bone continuum mechanics to the observed bone structure (Beaupré *et al.*, 1990b; Carter, 1987; Carter *et al.*, 1987; Cowin and Hegedus, 1976; Hart and Davy, 1989; Huiskes *et al.*, 1987; Kummer, 1972). Generally, stress-related internal bone remodeling theories take the form of an expression for the local time rate-of-change of bone density as a nonlinear function of mechanical quantities such as stress, strain, or strain energy density. The numerical implementation of these relationships with the finite element method allows simulation of the continuum level morphology and morphological changes a bone will undergo due to loading.

Carter *et al.* (1989) observed that when their simulation of femoral bone remodeling was allowed to progress past the first few iterations, 'The method employed appears to be converging toward a condition in which most of the elements will either be saturated . . . or be completely resorbed.' In particular, we and others (Harrigan and Hamilton, 1992; Weinans *et al.*, 1992a) have observed that previous bone remodeling implementations tend towards discontinuous density patterns. In regions (e.g. the diaphysis of long bones) discontinuous cortical structures are predicted that match well with the observed morphology. However, close to the applied loads, alternating patterns of high and low density elements were predicted that resemble a checkerboard.

We propose that a single bone remodeling formulation can describe the development and maintenance of both types of morphology (continuous and discontinuous). In particular, such a formulation would predict discontinuous structures when applied to the simple load resultants experienced in the diaphysis (what we will term 'far-field' behavior), and

Received in final form 28 May 1994.
Address correspondence to: Chris Jacobs, Dept. of Orthopaedics, P.O. Box 850; 500 University Drive, Hershey, PA 17033, U.S.A.

yet could be driven to a continuous structure when applied to the more complex loading found near the joints (what we will term 'near-field' behavior).

We propose that in the near-field case, the current continuum equations indeed lead to continuous densities, but that a numerical difficulty associated with the finite element discretization introduces the anomalous checkerboard density pattern. In other works, the current continuum formulation is able to model both the far-field discontinuous result as well as the near-field continuous result, but in the near-field case, the numerical procedure admits a spurious 'checkerboard' mode that is not inherently present in the continuum formulation. Therefore, a single biologic adaptation mechanism may be responsible for both cortical and trabecular bone structures as well as the transition between these structures as it is seen in long bones.

METHODS

Trabecular bone is a porous structure and, given current computing resources, stress analysis of whole bones can only be carried out on an 'average' or continuum level (Harrigan *et al.*, 1988). Much progress has been made in direct modeling of cancellous microstructure (Fyhrie and Hamid, 1993; Fyhrie *et al.*, 1992), but to date these techniques have not advanced sufficiently to model individual trabeculae in a whole bone simulation. Thus, both the mechanical variables and the biological response must be spatially averaged to yield appropriate apparent continuum variables (Aoubiza *et al.*, 1992; Hollister *et al.*, 1992) that can be used in a mathematical description of mechanically induced bone remodeling. In this paper we will confine ourselves to formulations where the homogenized continuum stress is related to the average trabecular stress through a power of the apparent density. It has been shown that the particular form of this scaling has a dramatic influence on the predicted remodeling behavior (Harrigan and Hamilton, 1992).

In this paper we explore the behavior of the remodeling formulation advanced by Beaupré *et al.* (1990b) as a particular example of strain-energy-based remodeling theories (see Appendix). According to these authors bone is assumed to respond to changes in a daily tissue level stress stimulus, Ψ_b , such that:

$$\begin{aligned} \frac{d\rho}{dt} &= A(\Psi_b - \Psi_{bAS})S_v(\rho), \quad 0 \leq \rho \leq \rho_c, \\ \frac{d\rho}{dt} &= 0, \quad \text{otherwise,} \end{aligned} \quad (1)$$

where ρ is the volumetric mass density (apparent density), ρ_c is the maximum observed density of cortical bone, Ψ_{bAS} is the constant level of daily tissue level stress stimulus that will result in no net change in bone density (termed the *attractor state stimulus*), A is a rate constant or function and may or may not include a dead-zone effect, and S_v is the surface area per unit volume at the current density (based upon an empirically determined fifth-order polynomial in porosity (Martin, 1984)). In this model the daily tissue level stress stimulus is defined as

$$\Psi_b = \left(\sum_{\text{day}} n_i \bar{\sigma}_{bi}^m \right)^{1/m}, \quad (2)$$

where n_i is the number of daily cycles of load type i , $\bar{\sigma}_{bi}$ is a tissue level effective stress scalar, and the stress exponent, m , is an empirical constant. To be useful for bone remodeling simulation, Ψ_b in equation (1) must be scaled from continuum level quantities (Carter *et al.*, 1987). By assuming that this scaling takes the same form as ultimate stress (Carter and Hayes, 1977) we have

$$\begin{aligned} \frac{d\rho}{dt} &= A \left(\Psi \left(\frac{\rho_c}{\rho} \right)^2 - \Psi_{bAS} \right) S_v(\rho), \quad 0 \leq \rho \leq \rho_c, \\ \frac{d\rho}{dt} &= 0 \quad \text{otherwise,} \end{aligned} \quad (3)$$

where

$$\Psi = \left(\sum_{\text{day}} n_i \bar{\sigma}_i^m \right)^{1/m} \quad (4)$$

is the continuum level effective stress stimulus, $\bar{\sigma}_i = \sqrt{2EU_i}$ is the continuum level effective stress, E is the average Young's modulus, and U is the continuum level strain energy density.

Finally, density changes must be related to changes in material properties. Generally, an empirically derived relationship between density and material properties is employed. A common form is that of linear isotropic elasticity such that

$$E = D\rho^n, \quad (5)$$

(Carter and Hayes, 1977), where E is the Young's modulus and D and n are experimentally derived parameters (which may vary with density) with n usually ranging from two to three. This relation has been refined to yield better agreement with current experimental evidence as it becomes available. However, the results described here are insensitive to the exact form of equation (5). As a result of equation (5) the matrix of elastic constants, C , in the linear elastic constitutive equation

$$\sigma = C(\rho) : \varepsilon \quad (6)$$

depends on density which implicitly depends on the stress and strain history. Equations (3), (4), (5) and (6), together with the equilibrium equation, make up a rate-dependent nonlinear continuum model for bone remodeling. With prescribed tractions or displacements on the boundaries and initial conditions for the density, the problem is in principle properly defined and may be solved numerically.

Traditionally a very straightforward method is applied to numerically solve the remodeling equations with the finite element method. The procedure is based on the approximation that each element has a uniform density. The element densities become state variables that determine the current configuration of the model (Fig. 2(a)). From one model configuration, the solution is advanced in time by solving the elasto-static problem using the known density distribution with the finite element method. The required mechanical variable (e.g. strain-energy density) is then computed at each element centroid by averaging the results from the integration points. The model configuration is advanced using the density rate-of-change from the remodeling theory and a time stepping algorithm (typically forward Euler). This strategy falls within the conventional finite element treatment of inelastic continuum models (Simo and Hughes, 1992).

This approach is 'element-based' in the sense that bone density is computed at element centroids and then assumed to be constant throughout the element. The traditional approach from computational inelasticity would be to use the densities at the integration points as state variables (Fig. 2(b)). Also, one might increase the order of interpolation of the displacements (Fig. 2(c)), with the corresponding increase in the number of integration points. Our approach was to use a 'node-based' implementation. Accordingly we applied equation (3) and kept track of the resulting density predictions at nodes rather than element centroids (Fig. 2(d)). Material properties, and therefore densities, are required at the integration points to perform conventional gauss-quadrature and assemble the finite element stiffness matrix. By interpolating nodal density values over the element interiors using the element shape functions, the integration point densities were computed. This is entirely analogous to the standard interpolation of nodal displacements or

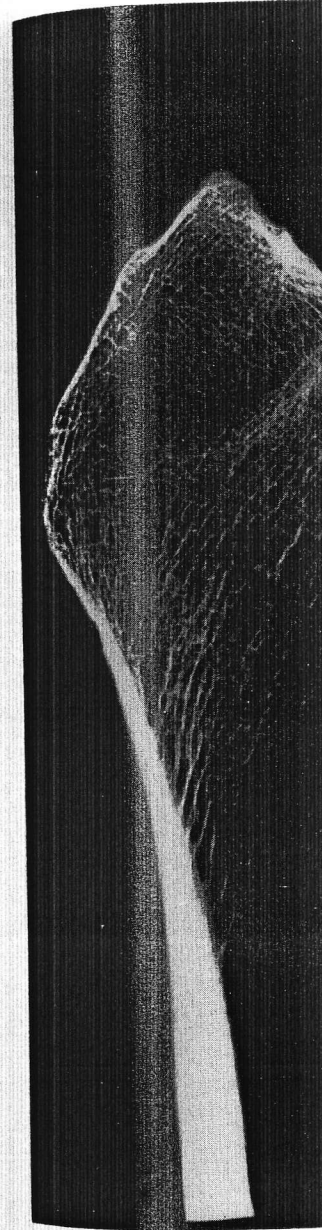


Fig. 1. This contact radiograph of a primarily cortical bone distally to a single mathematical formulation of recently been raised due to the observed discontinuous structures, and do not

$$-\Psi_{\text{BAS}}) S, (\rho), \quad 0 \leq \rho \leq \rho_c,$$

se,

(3)

$$= \left(\sum_{\text{day}} n_i \bar{\sigma}_i^m \right)^{1/m}$$

(4)

fective stress stimulus, $\bar{\sigma}_i = \sqrt{2EU_i}$ is
 ctive stress, E is the average Young's
 ntinuum level strain energy density.
 ges must be related to changes in
 ically, an empirically derived rela-
 ty and material properties is em-
 i is that of linear isotropic elasticity

$$E = D\rho^n, \quad (5)$$

), where E is the Young's modulus
 nentially derived parameters (which
 with n usually ranging from two to
 been refined to yield better agree-
 mental evidence as it becomes avail-
 lts described here are insensitive to
 n (5). As a result of equation (5) the
 ts, C , in the linear elastic constitutive

$$\sigma = C(\rho) : \varepsilon \quad (6)$$

ch implicitly depends on the stress
 ations (3), (4), (5) and (6), together
 uation, make up a rate-dependent
 odel for bone remodeling. With pre-
 placements on the boundaries and
 density, the problem is in principle
 ay be solved numerically.

traightforward method is applied to
 odeling equations with the finite
 ocedure is based on the approxima-
 as a uniform density. The element
 ariables that determine the current
 el (Fig. 2(a)). From one model con-
 is advanced in time by solving the
 ing the known density distribution
 method. The required mechanical
 y density) is then computed at each
 raging the results from the integra-
 nfiguration is advanced using the
 from the remodeling theory and
 hm (typically forward Euler). This
 onventional finite element treat-
 num models (Simo and Hughes,

ment-based' in the sense that bone
 element centroids and then assumed
 out the element. The traditional ap-
 onal inelasticity would be to use the
 ration points as state variables
 ght increase the order of interpola-
 s (Fig. 2(c)), with the corresponding
 of integration points. Our approach
 d' implementation. Accordingly we
 d kept track of the resulting density
 rather than element centroids
 roperties, and therefore densities, are
 ion points to perform conventional
 ssemble the finite element stiffness
 g nodal density values over the el-
 element shape functions, the integra-
 e computed. This is entirely analog-
 rpolation of nodal displacements or

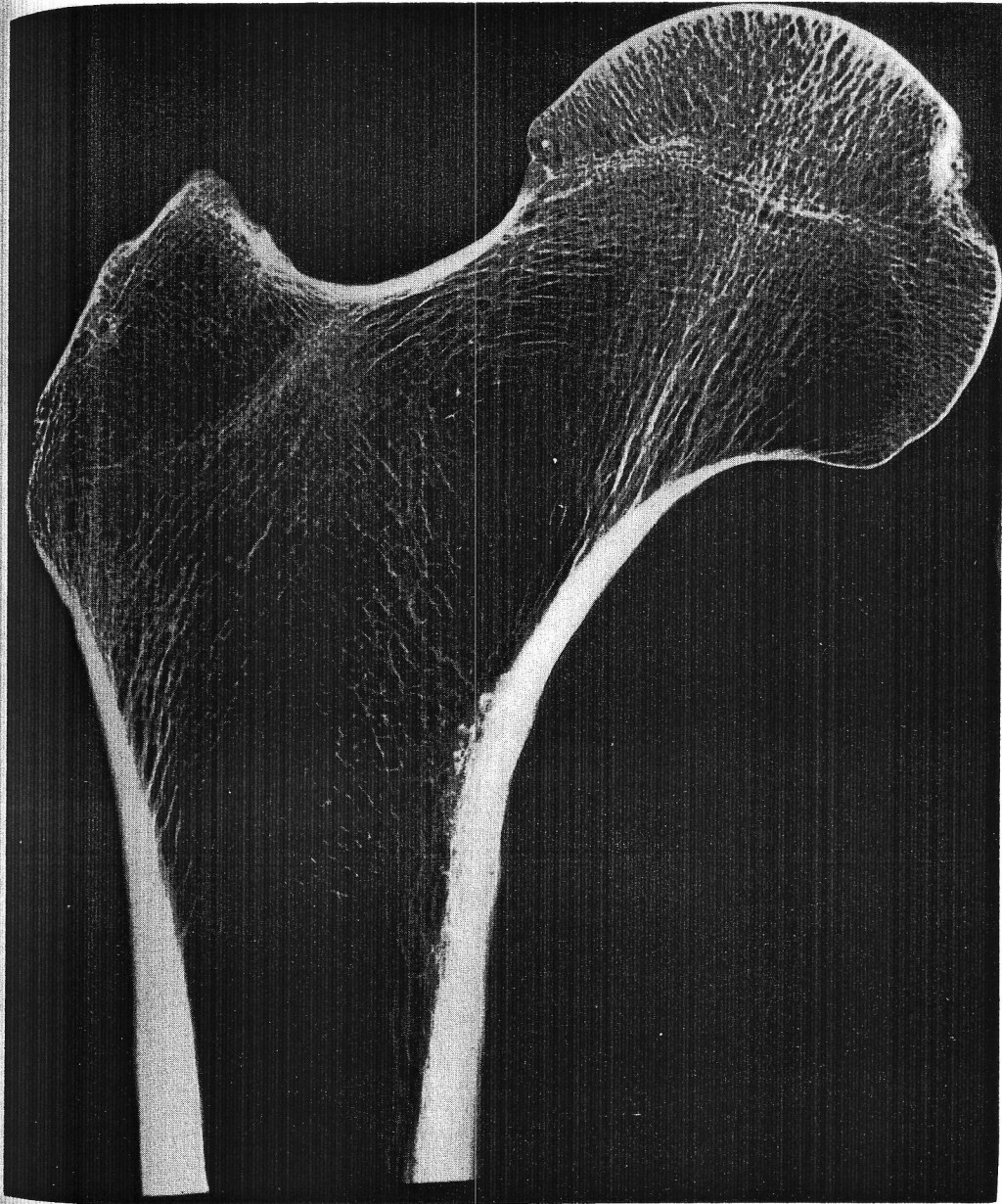


Fig. 1. This contact radiograph of a coronal slice through the proximal femur clearly shows the dramatic transition from primarily cortical bone distally to primarily trabecular bone proximally. The hypothesis investigated in this work is that a single mathematical formulation of adaptive bone remodeling can produce both types of bony structure. Some doubt has recently been raised due to the observation that current mathematical formulations seem to have a predisposition towards discontinuous structures, and do not seem to be capable of predicting the continuous apparent densities observed in the femoral head and neck regions.

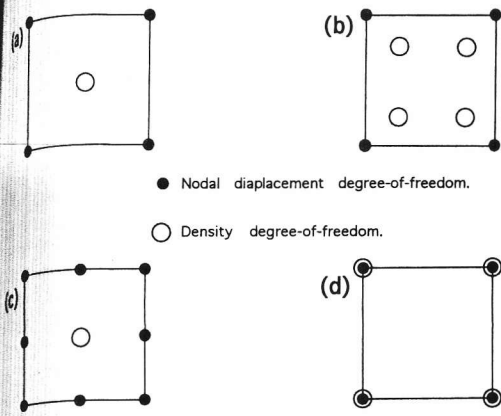


Fig. 2. The displacement and density interpolation schemes for the various methods are shown schematically for a quadrilateral parent element: (a) the common element-based approach; (b) traditional inelasticity approach; (c) higher-order element-based approach; (d) proposed node-based approach. The fundamental distinction between the methods is the location of displacement and density degrees of freedom, which is denoted by the closed and open circles respectively. Each implementation will be evaluated, in turn, for its ability to predict continuous near-field results, while maintaining cortical structures in the far-field case.

temperatures. Density continuity is ensured across element boundaries in the same way that it is for displacements. The only difficulty with implementing this approach is that the stress and strain quantities needed to apply equation (3) are not unique at the nodes. That is, most elasto-static elements employ piecewise continuous (C^0) interpolation functions. This leads to discontinuities in stress and strain at element boundaries. To overcome this, one of many smoothing techniques must be employed (Hughes, 1987, Section 4.4.1; Lee *et al.*, 1979; Lee and Gresho, 1978). In our case, the strain-energy-density was extrapolated from the integration points to the nodes by inverting the bilinear nodal interpolations within each element. The contributions at each node were then averaged (this is accomplished automatically by ABAQUS when nodal averaged results are requested). This technique can be shown to be equivalent to a least-squares (L_2) projection to the nodes similar to the one used by many finite element post-processors when plotting contours of elemental results.

Incremental calls to the commercial finite element code ABAQUS (v4.9, running on an HP/Apollo 9000 Model 730 workstation) were made in which the current material configuration was specified in the form of the current bone density at each node together with a table of values relating density to material properties (Young's modulus and Poisson's ratio). As the stiffness matrix was assembled, the density values were interpolated from the nodes to the integration points. The material table was then used to obtain

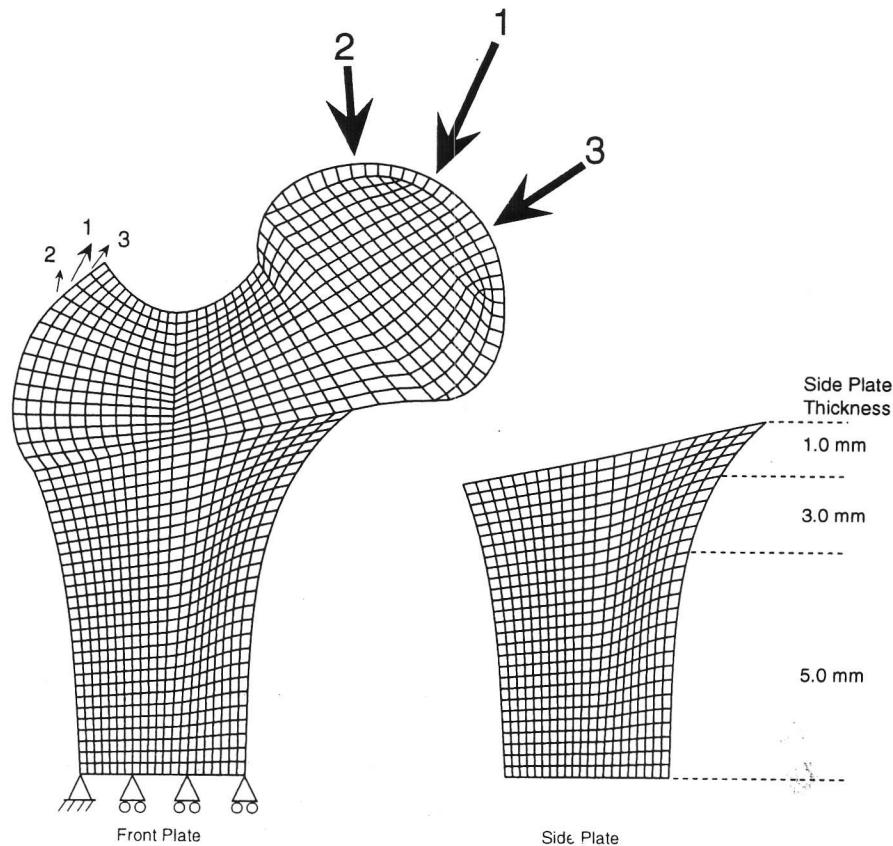


Fig. 3. The two-dimensional proximal femur model used to study the stability of bone remodeling algorithms employed the external geometry and loading of Beaupré *et al.* (1990a). A side-plate of cortical bone was coupled to the distal portion to account for the three-dimensional connectivity of the cortex. The side-plate and front-plate were connected via the three lateral and medial most nodes along each edge. The front-plate was assumed to be 40.0 mm thick. The side-plate was not allowed to remodel. Three cyclically applied load cases were selected to characterize a typical loading history. Six thousand cycles of load case one and two thousand cycles of load cases two and three were applied. The bottom edge was supported on rollers with the left-most node fully constrained to eliminate lateral rigid-body translations.

material properties. After a solution had been obtained, the results reported at nodes were used to advance the solution to the next time increment through numerical integration of equation (3) at the nodes. Forward Euler integration was used and the time step was selected to be well below the stability limit (Beaupré *et al.*, 1990a; Orr, 1990).

We considered four finite element implementations (Fig. 2) as follows: element-based with bilinear elements, integration-point-based with bilinear elements, element-based with bi-quadratic elements, and node-based with bilinear elements. Each of the four methods was applied to the example finite element problem in turn (Fig. 3). A side-plate of cortical bone of varying thickness was used to account for the three-dimensionality of the cortical structures in the proximal femur (Weinans *et al.*, 1992b). In each case, the simulation was started with a homogeneous distribution of an intermediate density (0.6 g cm^{-3}). A linear rate-relation was used in these simulations with the rate constant taken from Beaupré *et al.* (1990a). All of the simulations were carried out for a large enough period of time (500 ten-day increments) for density changes to approach zero (the largest change in density for the final time increment was less than 0.01 g cm^{-3} in all cases) in order for the spatial stability of each method to become fully evident. In each case, the resulting density predictions were plotted directly as predicted by the appropriate interpolation functions. That is, no smoothing from the post-processor has taken place. Finally, for reference purposes, the results from the traditional element-centroid method (Fig. 2(a)) were used to produce a traditional contour plot after the density data had been projected onto the nodes.

RESULTS

The phenomena which raised the initial biological question is clearly demonstrated by the results of the traditional



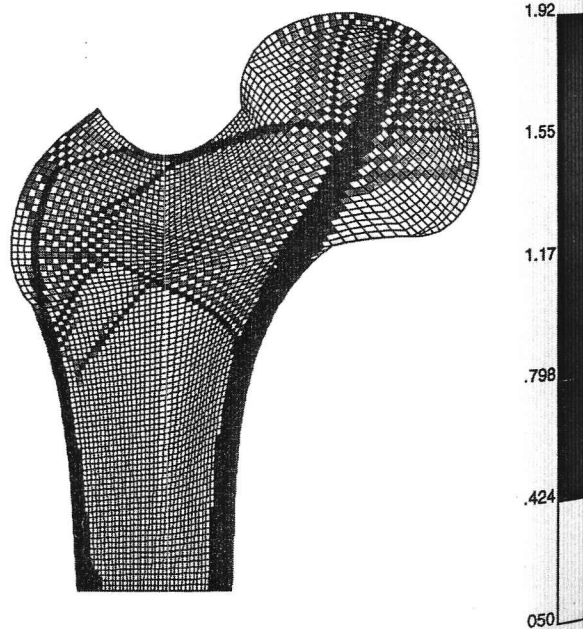
4

Fig. 4. The density distribution resulting from a bone remodeling simulation carried out using the traditional element-based algorithm (Fig. 2(a)). This type of behavior is clearly nonbiological in nature and motivates the question: are the current strain-energy-based continuum formulations incapable of predicting the expected continuous results near bone ends (and thus, biologically inappropriate), or is this difficulty technical in nature to be overcome with appropriate numerical implementation? Note that far from the region of applied load, strut-like structures develop the appropriately emulate the cortical structures seen in the diaphyses. On the other hand, in the proximal region of the model an anomalous checkerboard pattern of density develops. Upon refinement, note that the cortical structures remain intact, while the checkerboard pattern is clearly mesh dependent, at least at this level of refinement.

centroidal method (Fig. 4), which also clearly shows the formation of cortices far from the applied load. In this region, the predicted morphology agrees well with observed morphology. However, near the applied load we see the formation of the alternating checkerboard pattern. Note that upon refinement of the mesh, the checkerboard remains. Where there was one element of a certain density in the coarser mesh, there are now four elements of alternating density in the refined mesh. This mesh dependency suggests that the discontinuities in this region result from the numerical procedure employed.

Furthermore, the second two numerical techniques investigated (Fig. 2(b) and (c)) failed to yield the biologically expected continuous result. In the case of densities computed at integration points (Fig. 5), the checkerboard pattern once again occurred. However, there were very large density gradients superimposed on top of the original pattern which results in predicted densities that violate the density limits imposed by the remodeling theory when they are extrapolated throughout the element interior, although each individual density is within the density bounds of zero and cortical bone. When eight-noded elements were used, the density distribution seems more appropriate (Fig. 6). Notice that the checkerboard pattern has been greatly suppressed, although some discontinuities remain in the femoral head and neck regions where they are not observed anatomically.

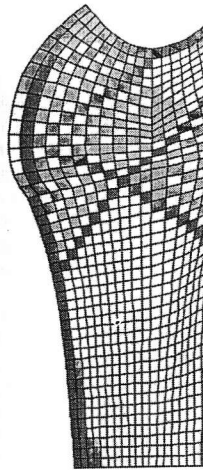
The results for the nodal method (Fig. 7) support the hypothesis that a single mathematical model may indeed describe both continuous and discontinuous structures simultaneously, and that current strain-energy-based continuum formulations like the one employed here are capable of just that. Specifically note that in regions where the interaction between the remodeling equations and the finite element discretization had produced the checkerboard patterns (Fig. 4) we find continuous distributions of intermediate densities. Furthermore, the formation of cortices far from the region of load application is maintained indicating that both



6

Fig. 6. Using a higher-order element formulation, significant discontinuities in the femur are suppressed, resulting in a more continuous density distribution.

stable and unstable behavior (i.e., continuous predicted density distribution) to biological adaptation, depend on local loading conditions.

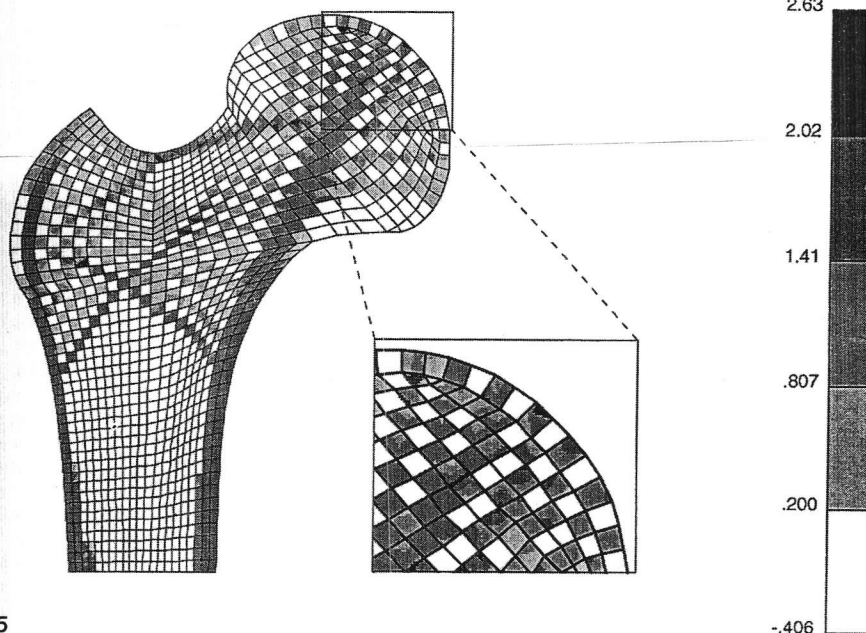


5

Fig. 5. If the remodeling equation density gradients are predicted across the element-based procedure have densities from the integration point

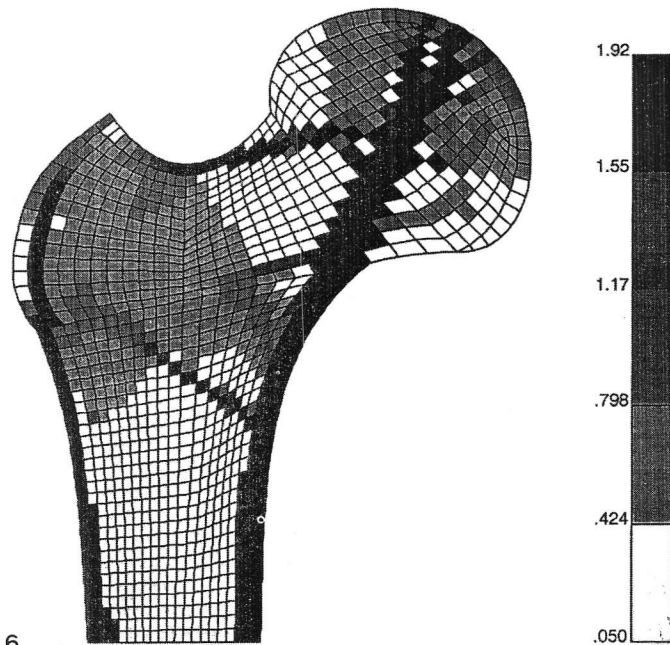
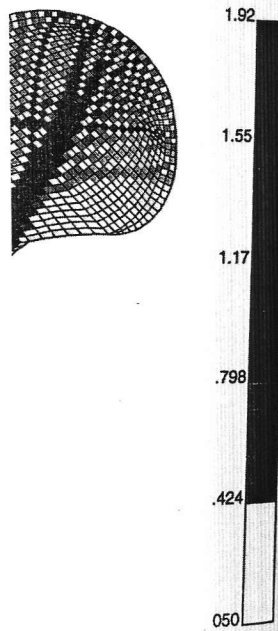
Fig. 4), which also clearly shows the far from the applied load. In this morphology agrees well with observed r, near the applied load we see the checkerboard pattern. Note that the mesh, the checkerboard remains element of a certain density in the re now four elements of alternating mesh. This mesh dependency suggests in this region result from the numer-

second two numerical techniques investigated (c) failed to yield the biologically result. In the case of densities computed (Fig. 5), the checkerboard pattern since ver, there were very large density on top of the original pattern which isities that violate the density limits eling theory when they are extrapolated element interior, although each indi- n the density bounds of zero and ght-noded elements were used, the ns more appropriate (Fig. 6). Notice pattern has been greatly suppressed. nities remain in the femoral head they are not observed anatomically. nodal method (Fig. 7) support the : mathematical model may indeed is and discontinuous structures si- current strain-energy-based con- the one employed here are capable note that in regions where the inter- deling equations and the finite el- duced the checkerboard patterns ous distributions of intermediate e formation of cortices far from the is maintained indicating that both



5

Fig. 5. If the remodeling equations are applied at integration points rather than element centroids (Fig. 2(b)) very large density gradients are predicted across element interiors. When these results are compared with Fig. 4 it is clear that the global density distribution has not been significantly altered. Instead, elements that had remodeled to a constant density value using the element-based procedure have large density gradients with roughly the same average density. Extrapolating the bone densities from the integration points throughout the element interiors, yield densities which violate the physical limitations on porosity.



6

Fig. 6. Using a higher-order element-based formulation (see Fig. 2(c)) eliminates much of the checkerboarding. However, significant discontinuities in the femoral head and neck region remain. This approach requires a much greater investment of computational resources with no resulting refinement in the predicted density distribution.

g the traditional element-based s the question: are the current us results near bone ends (and e with appropriate numerical the appropriately emulate the el an anomalous checkerboard while the checkerboard pattern

stable and unstable behavior (i.e. continuous and discontinuous predicted density distributions) can occur regionally due to biological adaptation, depending on the character of the local loading conditions.

Finally, to facilitate a comparison of our results with those in the literature, a nodal projection and contour plot was prepared from the data predicted with the element-based method applied to the four-node mesh (Fig. 8).

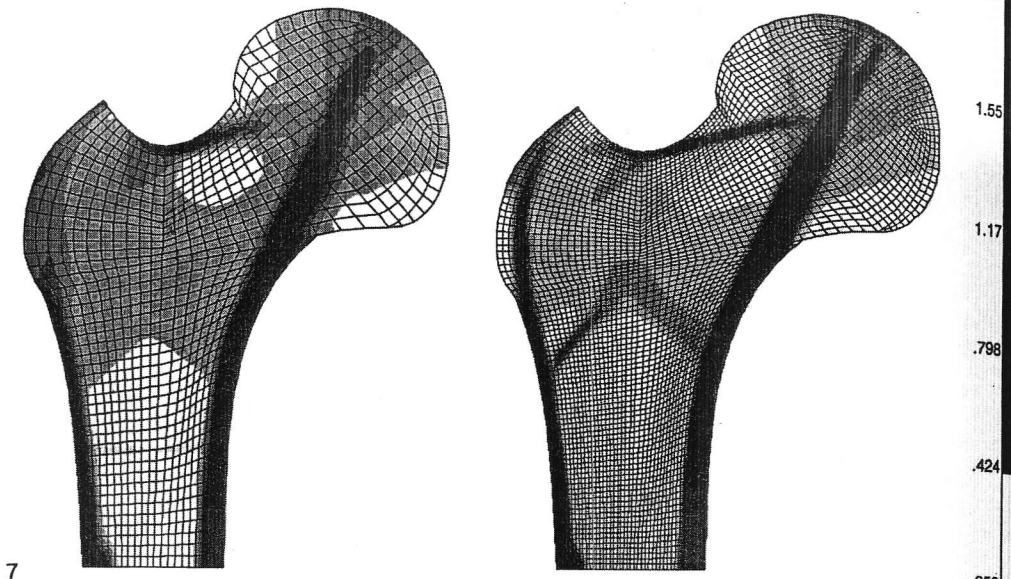


Fig. 7. The density distribution resulting from the node-based method. Although this is a contour plot, no smoothing from the post-processor has occurred. Notice that the checkerboarding has been replaced by a continuous density distribution. Strut formation far from the load application is still found and the cortical structures drop to a low density in the intramedullary space across one element. These results support the interpretation that the current continuum formulation yield appropriately continuous solutions in near-field loading situations, and that previously observed discontinuities occur due to purely numerical considerations. This, in turn, supports the biologic hypothesis that the same adaptive bone remodeling mechanism that leads to discontinuous cortical structures can also produce continuous cancellous structures. Refining the mesh reveals more details of the internal femoral structure (note the intriguing bifurcation near the joint surface).

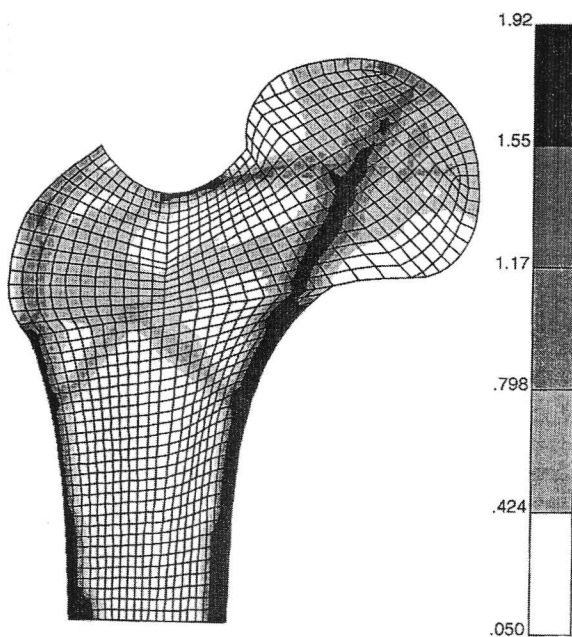


Fig. 8. For comparison, the element centroid densities from the final iteration of the element-based approach, using the coarse mesh (Fig. 4), were projected to the nodes and a contour plot was prepared. This was accomplished via the 'fringe plot' option in Patran. Note that the result is quite similar to Fig. 7, indicating that the bulk of the simulations currently in the literature do not need to be re-analyzed.

DISCUSSION

We have shown that a single mathematical description of continuum level adaptive bone remodeling can lead to both continuous far-field behavior and continuous near-field behavior, which supports the proposal that the same mechanical biological adaptive mechanisms are involved in the formation and maintenance of both type of structures. To see how this is possible, notice that the stress stimulus term in equation (3) will in general depend on the global density distribution because the local stress and strain (which determine the stress stimulus) are influenced by remote changes in density. Thus, the continuum equations may have continuous solutions in one case and discontinuous solutions in another case depending on how the local stress and strain depend on the global density distribution. In fact, in all but the simplest of cases, it is extremely difficult or impossible to determine the continuity of the continuum solution, since analytical solutions of the complete nonlinear rate-dependent problem are not available.

Weinans *et al.* (1992) studied the simplified far-field example of an axial resultant load. Harrigan and Hamming (1992) investigated continuum solutions as well as numerical solutions (the similarities between the formulation used in these studies and the Beaupré *et al.* (1990b) formulation are explored in the Appendix). Both of these studies found the system to be spatially unstable, which agrees well with the far-field results found here. This configuration is an accurate model of the mechanical environment of the mid-shaft region of most long bones far from the applied load and is what we have termed the 'far-field' behavior. In this region we do not find any intermediate values of density, thus the continuum equations agree well with observations.

However, in regions where the local loading conditions are sufficiently complex, these conclusions may not apply

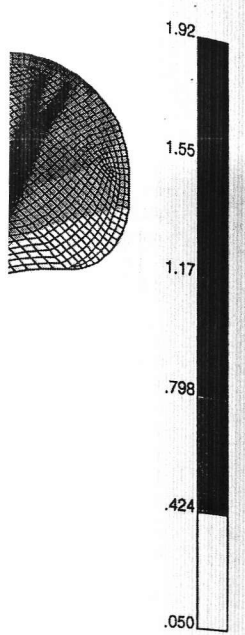
since the relation between local stress and global density distribution may be quite different. The continuum solution to be a continuous distribution adjacent to applied distributed loads is impossible to ignore end effects and is well known as 'near-field' behavior. In the region near the joint surface an alternating pattern of bone densities is observed. The results of traditional methods (Fig. 4) have been termed a 'patchwork' (Weinans) or a 'checkerboard' pattern (Jacobs). Unlike the far-field discontinuities, this behavior is mesh-dependent and strikingly reminiscent of instabilities arising in marginally stable finite element formulations (Simo and Armero, 1992). In the present formulation, discontinuities seem to arise due to an interaction between the remodeling equations and the discrete numerical method used to simulate them.

Another approach is to apply the remodeling equations and update density changes at integration points rather than at element centroids. This implementation is a standard finite element implementation of the theory of inelasticity (Simo and Hughes, 1992). However, due to the bone remodeling equations, the density gradients across element interfaces are continuously changing the global solution (Fig. 7).

Higher-order elements may be employed to produce better numerical performance. However, if the remodeling equations are applied at the nodes, large density gradients are found. If the remodeling equations are applied at the element centroids of higher-order elements, the near-field discontinuities are eliminated and a smooth density pattern is observed. However, this is a sub-optimal element (Hughes, 1987) and a large number of displacement degrees-of-freedom are associated with an increased level of density. The result presented here is the most efficient displacement degrees of freedom compared to a mesh with four-node elements. This leads to better performance and wasted computer resources. This may not seem to be a crucial issue, but it is in mind that as finite element models become more refined and particularly when they are used in high dimensions, computational efficiency becomes a consideration.

Certain interesting parallels exist between the present simulation and the finite element method with other nonliving nonadapting materials. These parallels help to relate the approach to the broad number of approaches associated with the finite element method implementations in general. Several of the finite element formulations for incompressible materials exhibit spurious pressure modes (Hughes, 1987; Strang and Fix, 1973). This difficulty with checkerboard pressure modes introduces a numerical instability that are not present in the present formulation. A common solution is to use an average density (Hughes, 1987, Section 4.4.1; Levenberg). Although somewhat *ad hoc* in nature, the use of pressure-smoothed elements are a good approximation to the continuum behavior. Essentially the same approach to smooth the discontinuities is used in the present formulation in computing the nodal density needed in the node-based bone remodeling simulation.

Bone remodeling simulation is also a simulation of materials that have a plastic behavior in the plastic region. These are the present numerical difficulties that have been observed in reformulating the continuum equations. In the local formulation (where the material



four plot, no smoothing from continuous density distribution. In the present continuum formulations observed discontinuities occur that the same adaptive bone structures near the joint surface.

DISCUSSION

The mathematical description of bone remodeling can lead to discontinuous near-field behavior. It is possible that the same mechanisms are involved in the formation of structures. To see how the stress stimulus term depends on the global density stress and strain (which determined by remote changes in the bone) may have continuous discontinuous solutions in the local stress and strain distribution. In fact, in all but the most difficult or impossible to obtain a continuum solution, since the complete nonlinear rate-dependence

of the simplified far-field loading. Harrigan and Hamilton solutions as well as numerical solutions between the formulation used in the present study and the formulation of the mid-shaft region applied load and is what we observe. In this region we do not observe density, thus the continuum solutions. The local loading conditions conclusions may not apply

since the relation between local stress and strain and the global density distribution may be quite different. We expect the continuum solution to be a continuous apparent density distribution adjacent to applied distributed loads where it is impossible to ignore end effects and is what we have termed 'near-field' behavior. In the region near the load application an alternating pattern of bone densities is seen in the numerical results of traditional methods (Fig. 4). This type of behavior has been termed a 'patchwork' (Weinans *et al.*, 1992a) or a 'checkerboard' pattern (Jacobs and Beaupré, 1992). Unlike the far-field discontinuities, this behavior is clearly mesh-dependent and strikingly reminiscent of numerical instabilities arising in marginally stable finite element methods (Simo and Armero, 1992). In the present context the discontinuities seem to arise due to an interaction between the remodeling equations and the discrete nature of the numerical method used to simulate them.

Another approach is to apply the remodeling relations and update density changes at integration points rather than at element centroids. This implementation is analogous to a standard finite element implementation of computational elastostatics (Simo and Hughes, 1992). However, when applied to the bone remodeling equations, this introduces large density gradients across element interiors without significantly changing the global solution (Fig. 5).

Higher-order elements may be employed in the hope of producing better numerical performance. As with linear elements, if the remodeling equations are applied at the integration points, large density gradients across element interiors are found. If the remodeling equations are applied at the element centroids of higher-order elements it is possible to eliminate the near-field discontinuities and produce acceptable density patterns. However, this technique leads to a sub-optimal element (Hughes, 1987) since the increased number of displacement degrees-of-freedom are not associated with an increased level of density refinement. To achieve the result presented here the model contained 10,758 displacement degrees of freedom compared with 3670 for the mesh with four-node elements. This leads to poor numerical performance and wasted computer resources. On the surface, this may not seem to be a crucial issue since acceptable solutions may be obtained with this method. However, keep in mind that as finite element models become more and more refined and particularly when they are extended to three dimensions, computational efficiency can become a critical consideration.

Certain interesting parallels exist between bone remodeling simulation and the finite element implementations used with other nonliving nonadapting materials. Illustrating these parallels helps to relate the approach presented here to the broad number of approaches associated with finite element implementations in general. Several mixed and penalty method formulations for incompressible materials lead to element formulations that exhibit rank-deficiencies which produce spurious pressure modes (Hughes, 1987, Appendix III; Strang and Fix, 1973). This difficulty exhibits itself as checkerboard pressure modes introduced by the numerical implementation that are not present in the continuum case. A common solution is to use an averaging procedure called 'filtering' (Hughes, 1987, Section 4.4.1; Lee and Gresho, 1978). Although somewhat *ad hoc* in nature, it can be shown that pressure-smoothed elements are a good approximation to the continuum behavior. Essentially we have adopted the same approach to smooth the discontinuous stress and strain quantities in computing the nodal strain energy density needed in the node-based bone remodeling implementation.

Bone remodeling simulation is also strikingly similar to the simulation of materials that have a strain softening behavior in the plastic region. These unstable materials also present numerical difficulties that have led investigators to reformulate the continuum equations. In particular, a nonlocal formulation (where the material behavior at a point

depends on the stress and/or strain in some surrounding region) has been recently employed (Brekelmans, 1993). In the field of bone remodeling simulation, two reformulations have been suggested recently; an adjustment of the parameters used in the model (leading to a stable material formulation) (Harrigan and Hamilton, 1992), and a nonlocal formulation (Mullender *et al.*, 1993). Both approaches can lead to acceptable density distributions and are certainly worth consideration. However, reformulation of the continuum equations should primarily be undertaken in order to model biological processes more faithfully, rather than being motivated by convenient numerical behavior once they have been discretized.

The node-based implementation described here seems to overcome the numerical difficulties of the near-field behavior associated with the original finite element implementation of the continuum formulation, while maintaining the desired far-field discontinuous solutions in the sense that nodal densities predicted at adjacent nodes still change abruptly from the saturated cortical value to zero. Although the density interpolations used in this method are continuous for this transition, this does not imply that the method is not capable of representing discontinuous cortical structures. As with the displacement predictions near a material interface in a conventional elasto-static simulation, the predictions are only accurate at particular points, and the only way to get more information between these points is to refine the mesh. The element-based method may be more appealing in this regard since it will yield a density discontinuity at the element boundary, however both methods predict some sort transition between two points (a node or element centroid); the only way to get more information about the density transition is to refine the mesh.

It must be noted that several factors may mitigate the near-field numerical difficulties associated with an element-based implementation. Many investigators now incorporate a 'dead-zone' or 'lazy-zone' (Beaupré *et al.*, 1990a; Huiskes *et al.*, 1987) to better simulate the biologic response. This has the additional effect of slowing down or preventing the full development of the density discontinuous. Although it is important to include a lazy-zone in a more physiologic simulation, for our purposes it would have the effect of obscuring the discontinuities we are interested in observing.

In the results presented here, the simulations were continued for a very long time. Note that the formation of a dense cortical strut in the femoral head is a result of oversimplified loads applied for an extreme duration. In a more physiologic situation it would be unrealistic to assume that a simple set of three load cases can represent the load history over the very long term. Thus, in a clinical application (e.g. predicted density changes due to the altered loading induced by total hip replacement) the simulation duration may be too short for inappropriate near-field discontinuities to manifest themselves.

Also, in most cases a graphical post-processor is used to generate contour plots for visualization of results. When centroidal results are plotted by many post-processors they are first extrapolated to and averaged at the nodes. Also known as an L_2 -projection, this smooths the raw data, tending to obscure the near-field type of discontinuity. The method we have presented also depends on projecting the stress and strain data to the nodes at each time step (and therefore smoothing them). It is difficult to distinguish end configuration contour plots of the element-based approach (where smoothing of density takes place once at the end of the analysis) from the node-based approach (where smoothing of stress and strain take place at each time step). Thus, the bulk of the data in the literature is not likely to require reinterpretation.

In the node-based implementation, no features specific to ABAQUS have been employed. In fact, any code that can solve thermoelastic problems can be used by simply specifying a material with a temperature dependence, using the

density in place of temperature. At each increment one specifies the density distribution throughout the model where the code expects to find the temperature.

In this treatment, we have made a distinction between near-field and far-field bone remodeling behavior. Although the transition from cortical to trabecular morphology can be quite dramatic, this distinction is admittedly artificial. As a conceptual construction, however, it is helpful to express certain concepts of bone remodeling, namely that a single formulation can be used in both situations, as well as regions of transition from one to the other.

Long bone structure transitions from a primarily nonporous cortical form in the diaphysis to a highly porous trabecular form in the epiphyses. Many investigators have explicitly or implicitly suggested that this is an adaptation to changing mechanical demands in the two different regions, which suggests that a single biological mechanism of stress-adaptation may explain the formation of both types of bony morphology. We have presented evidence that currently employed continuum formulations of bone remodeling on the apparent level can produce both continuous and discontinuous solutions, depending on the character of the local mechanical loading, when appropriate numerical methods are employed. In this way, current formulations are attractive since they hypothesize a single strain-energy-based mechano-biologic mechanism which leads to continuous or discontinuous morphologies depending on the local loading environment. This property seems to agree well with the observation of two distinct types of bone (cortical and cancellous) which occur regionally in response to the local mechanical requirements. The node-based method for simulating bone remodeling has attractive properties in this area as well as computational efficiency and thus, we believe it to be the method of choice.

Acknowledgements—This work was supported by the Department of Veterans Affairs (Merit Review Project # A501-2RA) and the National Science Foundation for a graduate fellowship awarded to M.E. Levenston. Also, we would also like to acknowledge the San Diego Supercomputer Center, PDA Engineering (Costa Mesa, CA 92626) for an educational license for the use of Patran, and HKS Inc. (Pawtucket, RI 02860-4847) for an educational license for the use of ABAQUS.

REFERENCES

- Aoubiza, B., M. C. J., A. M. and L. S. (1992) A new process of mechanical characterization of compact bone. *Recent Advances in Computer Methods in Biomechanics & Biomedical Engineering* (Edited by Middleton, J., Pande, G. N. and Williams, K. R.), pp. 288-297. Swansea, Books and Journals International Ltd.
- Beaupré, G. S., Orr, T. E. and Carter, D. R. (1990a) An approach for time-dependent bone modeling and remodeling - application: a preliminary remodeling simulation. *J. orthop. Res.* **8**, 662-670.
- Beaupré, G. S., Orr, T. E. and Carter, D. R. (1990b) An approach for time-dependent bone modeling and remodeling - theoretical development. *J. orthop. Res.* **8**, 651-661.
- Breklemans, W. A. M. (1993) Nonlocal formulation of the evolution of damage in a one-dimensional configuration. *Int. J. Solids Struct.* **30**, 1503-1512.
- Carter, D. R. (1987) Mechanical loading history and skeletal biology. *J. Biomechanics* **20**, 1095-1109.
- Carter, D. R., Fyhrie, D. P. and Whalen, R. T. (1987) Trabecular bone density and loading history: regulation of connective tissue biology by mechanical energy. *J. Biomechanics* **20**, 785-794.
- Carter, D. R. and Hayes, W. C. (1977) The compressive behavior of bone as a two-phase porous structure. *J. Bone Jt Surg.* **59A**, 954-962.
- Carter, D. R., Orr, T. E. and Fyhrie, D. P. (1989) Relationships between loading history and femoral cancellous bone architecture. *J. Biomechanics* **22**, 231-244.
- Cowin, S. C. and Hegedus, D. H. (1976) Bone Remodeling: a theory of adaptive elasticity. *J. Elasticity* **6**, 313-326.
- Curry, J. (1984) *The Mechanical Adaptation of Bones*. Princeton University Press, Princeton.
- Fyhrie, D. P. and Hamid, M. S. (1993) The probability distribution of trabecular level strains for vertebral cancellous bone. *Trans. 39th ORS*, 175.
- Fyhrie, D. P., Hamid, M. S., Kuo, R. F. and Lang, S. M. (1992) Direct three-dimensional finite element analysis of human vertebral cancellous bone. *Trans. 38th ORS*, 551.
- Harrigan, T. P. and Hamilton, J. (1992) An analytic and numerical study of the stability of bone remodeling theories: dependence on microstructural stress transformations. *J. Biomechanics* **25**, 477-488.
- Harrigan, T. P., Jasty, M., Mann, R. W. and Hamid, W. H. (1988) Limitations of the continuum assumption in cancellous bone. *J. Biomechanics* **21**, 269-275.
- Hart, R. T. and Davy, D. T. (1989) Theories of bone modeling and remodeling. *Bone Mechanics* (Edited by S. C. Cowin), pp. 253-277. CRC Press, Boca Raton.
- Hollister, S. J., Brennan, J. M. and Kikuchi, N. (1992) Homogenization sampling analysis of trabecular bone microstructural mechanics. *Recent Advances in Computer Methods in Biomechanical & Biomedical Engineering* (Edited by Middleton, J., Pande G. N. and Williams, K. R.), pp. 308-317. Swansea, Books & Journals International Ltd.
- Hughes, T. J. R. (1987) *The Finite Element Method*. Prentice-Hall, Englewood Cliffs.
- Huiskes, R., Weinans, H., Grootenboer, H. J., Dalstra, M., Fudala, B. and Sloof, T. J. (1987) Adaptive bone-remodeling theory applied to prosthetic-design analysis. *J. Biomechanics* **20**, 1135-1150.
- Jacobs, C. R. and Beaupré, G. S. (1992) The role of multiple load histories in bone remodeling simulation. *Trans. 38th ORS*, 535.
- Kummer, B. K. F. (1972) Biomechanics of bone: Mechanical properties, functional structure, functional adaptation. *Biomechanics* (Edited by Y. C. Fung), pp. 237-271. Prentice-Hall, Englewood Cliffs.
- Lee, R. L. and Gresho, P. M. (1978) Numerical smoothing techniques applied to some finite element solutions of the Navier-Stokes equations. *Second International Conference on Finite Elements in Water Resources*.
- Lee, R. L., Gresho, P. M. and Sani, R. L. (1979) Smoothing Techniques for certain primitive variable solutions of the Navier-Stokes equations. *Int. J. Num. Meth. Engng* **14**, 1785-1804.
- Martin, R. B. (1984) Porosity and specific surface of bone. *CRC Critical Reviews in Biomedical Engineering*, Vol. 16, pp. 179-222. CRC Press, Boca Raton.
- Mullender, M. G., Huiskes, R. and Weinans, H. (1993) A physiological approach to the simulation of bone remodeling. *Trans. 39th ORS*, 531.
- Orr, T. (1990) The role of mechanical stresses in bone remodeling, Ph.D. Thesis, Stanford University.
- Simo, J. C. and Armero, F. (1992) Geometrically non-linear enhanced strain mixed methods and the method of incompatible modes. *Int. J. Numer. Meth. Engng* **33**, 1413-1448.
- Simo, J. C. and Hughes, T. J. R. (1992) *Plasticity, Viscoplasticity, and Viscoelasticity: Formulation and Numerical Analysis Aspects*. Springer, Berlin.
- Strang, G. and Fix, G. J. (1973) *An Analysis of the Finite Element Method*. Prentice-Hall, Englewood Cliffs, NJ.
- Weinans, H., Huiskes, R. and Grootenboer, H. J. (1992a) The behavior of adaptive bone-remodeling simulation models.

APPENDIX

Weinans, H., Huiskes, R. and Grootenboer, H. J. (1992) Effects of material properties on femoral bone remodeling. *J. orthop. Res.* **10**, 100-108.

By assuming particular values for parameters in the remodeling formulation used in this paper we arrive at a formulation that is very similar to that of Weinans *et al.* (1992) and Harrigan and Hamid (1992). We assume that each load case is applied for a fixed number of cycles, N , and the stress exponent, m , becomes

$$\Psi = \sqrt{2NE \sum_{\text{day}} U}.$$

Next, if we assume that $n=3$ in equation (1), we become

$$\frac{d\rho}{dt} = A \left(\frac{\rho_c}{\rho} \right)^2 \sqrt{2ND\rho^3 \sum_{\text{day}} U} \times S_v(\rho), \quad 0 \leq \rho \leq \rho_c,$$

$$\frac{d\rho}{dt} = 0, \quad \text{otherwise.}$$

es, W. C. (1977) The compressive is a two-phase porous structure. 954-962.

and Fyhrie, D. P. (1989) Relation- ing history and femoral cancellous Biomechanics 22, 231-244.

us, D. H. (1976) Bone Remodeling t elasticity. J. Elasticity 6, 313-326. Mechanical Adaptation of Bones. Prin- s, Princeton.

mid, M. S. (1993) The probability ular level strains for vertebral cancellous bone. ORS, 175.

M. S., Kuo, R. F. and Lang, S. M. imensional finite element analysis of cellulous bone. Trans. 38th ORS, 551.

amilton, J. (1992) An analytic and ie stability of bone remodelling the microstructural stress transforma- s 25, 477-488.

l, M., Mann, R. W. and Harris, ons of the continuum assumption in Biomechanics 21, 269-275.

l. T. (1989) Theories of bone modeling e Mechanics (Edited by S. C. Cowin), ress, Boca Raton.

an, J. M. and Kikuchi, N. (1992) npling analysis of trabecular bone anics. Recent Advances in Computer ical & Biomedical Engineering (Edi- Pande G. N. and Williams, K. R.) pp ooks & Journals International Ltd. The Finite Element Method. Prentice- s.

H., Grootenboer, H. J., Dalstra, M. of, T. J. (1987) Adaptive bone-re- lled to prosthetic-design analysis. J. 35-1150.

pré, G. S. (1992) The role of multiple e remodeling simulation. Trans. 38th

2) Biomechanics of bone: Mechanical al structure, functional adaptation d by Y. C. Fung), pp. 237-271. Prentice-Hall, Englewood Cliffs.

l, P. M. (1978) Numerical smoothing o some finite element solutions of the ons. Second International Conference n Water Resources.

M. and Sani, R. L. (1979) Smoothing in primitive variable solutions of the ons. Int. J. Num. Meth. Engng 14,

porosity and specific surface of bone s in Biomedical Engineering, Vol II. Press, Boca Raton.

uiskes, R. and Weinans, H. (1993) A oach to the simulation of bone th ORS, 531.

ole of mechanical stresses in bone hesis, Stanford University.

o, F. (1992) Geometrically non-linear ed methods and the method of incom- l. Numer. Meth. Engng 33, 1413-1448.

s, T. J. R. (1992) Plasticity, Viscoplas- ticity: Formulation and Numerical. An- ger, Berlin.

l. J. (1973) An Analysis of the Finite Element Method. Prentice-Hall, Englewood Cliffs, NJ.

R. and Grootenboer, H. J. (1992a) The e bone-remodeling simulation models. 1425-1441.

Weinans, H., Huiskes, R. and Grootenboer, H. J. (1992b) Effects of material properties on femoral hip components on bone remodeling. J. orthop. Res. 10, 845-853.

APPENDIX

By assuming particular values for parameters in the re- modeling formulation used in this paper it is possible to arrive at a formulation that is very similar to those used by Weinans et al. (1992) and Harrigan and Hamilton (1992). If we assume that each load case is applied for an equal number of cycles, N , and the stress exponent, $m=2$, equation (2) becomes

$$\Psi = \sqrt{2NE \sum_{\text{day}} U}. \tag{A.1}$$

Next, if we assume that $n=3$ in equation (5), equation (3) becomes

$$\frac{d\rho}{dt} = A \left(\left(\frac{\rho_c}{\rho} \right)^2 \sqrt{2ND\rho^3 \sum_{\text{day}} U - \Psi_{\text{bas}}} \right) \times S_v(\rho), \quad 0 \leq \rho \leq \rho_c,$$

$$\frac{d\rho}{dt} = 0, \quad \text{otherwise.} \tag{A.2}$$

Ignoring the specific surface area effect and consolidating the constants yields

$$\frac{d\rho}{dt} = \hat{A} \left(\sqrt{\frac{\sum U}{\rho}} - \hat{k} \right) S_v(\rho), \quad 0 \leq \rho \leq \rho_c,$$

$$\frac{d\rho}{dt} = 0, \quad \text{otherwise.} \tag{A.3}$$

When this is compared with the formulation taken from Weinans et al. (1992),

$$\frac{d\rho}{dt} = B \left(\frac{1}{n} \sum_{i=1}^n U_i - k \right), \quad 0 \leq \rho \leq \rho_c,$$

$$\frac{d\rho}{dt} = 0, \quad \text{otherwise,} \tag{A.4}$$

it is clear that the two sets of equations (A.3 and A.4) are very similar. Thus, it is not surprising that the stability behavior of the method is also similar. The equations analyzed by Harrigan and Hamilton (1992a) are a restricted case of equation (A.4).